Journal of
Materials Chemistry C

ROYAL SOCIETY OF CHEMISTRY

PAPER

View Article Online
View Journal | View Issue

Published on 16 May 2014. Downloaded by University of Windsor on 22/08/2014 13:12:37.

Cite this: *J. Mater. Chem. C*, 2014, **2**, 5931

In situ photo-induced chemical doping of solution-processed graphene oxide for electronic applications†

K. Savva,[a] Y.-H. Lin,[b] C. Petridis,[cd] E. Kymakis,[d] T. D. Anthopoulos*[b] and E. Stratakis*[ae]

Received 27th February 2014
Accepted 11th May 2014

DOI: 10.1039/c4tc00404c

www.rsc.org/MaterialsC

We developed a photochemical method for the simultaneous reduction and doping of graphene oxide (GO) layers through ultraviolet laser irradiation in the presence of a dopant precursor gas. It is shown that a few seconds of irradiation is sufficient to dope the GO lattice, while the doping and reduction levels can be readily controlled upon variation of the irradiation time. Using this method, the simultaneous reduction and doping of GO with chlorine or nitrogen atoms is achieved and confirmed by Raman, FTIR and X-ray photoelectron (XPS) spectroscopy measurements. To demonstrate the potential of the approach for practical applications, the photochemical method was successfully employed for the *in situ* laser induced modification of prefabricated GO field effect transistors. Real time monitoring of the evolution of charge transport as a function of irradiation time reveals significant changes, a result attributed to the chemical modification of the GO lattice. The facile, rapid and room temperature nature of the photo-induced method proposed here provides unique opportunities for the cost-effective synthesis of bulk amounts of chemically modified GO for a wide range of applications spanning from transistors and sensors to transparent electrodes for lighting and photovoltaic cells.

Introduction

Graphene is a 2-dimensional (2D), zero bandgap material with unique morphological, mechanical, optical, thermal and electrical properties.[1,2] However, the majority of graphene's applications are hindered by the absence of a semiconducting bandgap. As a result, numerous methods have been developed to introduce dopants into the graphene's lattice and in this way to engineer its bandgap.[3–12] One alternative method to dope graphene involves the chemical functionalization of the graphene oxide (GO) lattice[13–19] – a route that could potentially provide access to novel and previously unexplored graphene derivatives. Unfortunately, most of the methods reported to date fail to demonstrate precise control over doping levels and exhibit poor yield or scalability, posing limits for practical applications. In addition, the high temperature processes often required are time-consuming but, more importantly, are not compatible with emerging temperature-sensitive technologies such as large-area plastic/printed electronics. Therefore the development of a simple, low-temperature and high-throughput method for controllable doping of graphene is highly desirable.

Here we report a novel, facile and room temperature methodology that can be used for controllable photochemical doping of GO. GO contains large numbers of functional oxygen groups (*e.g.* epoxy, hydroxyl, carboxyl, and carbonyl) that could potentially be exploited in order to photo-chemically tune its electrical properties. A successful photochemical event is realized by the light-induced partial removal of such functional groups and the subsequent insertion of hetero-atoms into the GO lattice.[20,21] To date, various laser irradiation approaches have been adopted for GO treatment and are reviewed in ref. 22. Of great interest is the laser induced reduction of the GO lattice[23] demonstrated to be suitable for the realization of flexible graphene electrodes[24] and tailoring of the GO bandgap.[25] Moreover lasers had been used for the *in situ* treatment of GO devices.[26] Finally, a recently published study[27] showed that femtosecond laser irradiation can be used for N doping of GO. Our method relies on precise photochemical reactions initiated by pulsed laser irradiation in the presence of a dopant precursor gas. It is rapid and efficient since a few nanosecond pulses are sufficient to induce doping levels of a few percent. By simple tuning of the laser parameters the exact doping level can be controlled with good reproducibility. The technique negates the need for high temperature post deposition steps and can provide access to the

[a] *Institute of Electronic Structure and Laser (IESL), Foundation for Research and Technology – Hellas (FORTH), Heraklion, 71003, Greece. E-mail: stratak@iesl.forth.gr*

[b] *Department of Physics & Centre for Plastic Electronics, Imperial College London, Blackett Laboratory, London SW7 2BW, UK. E-mail: thomas.anthopoulos@imperial.ac.uk*

[c] *Department of Electronic Engineering, TEI of Crete, Chania 73132, Crete, Greece*

[d] *Center of Materials Technology and Photonics & Electrical Engineering Department, Technological Educational Institute (TEI) of Crete, Heraklion, 71003, Greece*

[e] *Materials Science and Technology Department, University of Crete, Heraklion, 71003, Greece*

† Electronic supplementary information (ESI) available. See DOI: 10.1039/c4tc00404c

Published on 16 May 2014. Downloaded by University of Windsor on 22/08/2014 13:12:37.

synthesis of large quantities of doped graphene sheets with good control over the doping level, which is not readily realized by existing methods. Using this method, the simultaneous reduction and doping of GO with a few percent of chlorine or nitrogen atoms was realized following irradiation in the presence of Cl_2 or NH_3 gases, respectively. We show that upon photochemical doping chlorine and nitrogen atoms substitute GO defects located on the edges as well as in the plane of the GO lattice.[9,11,28] To demonstrate the applicability of the method for practical device applications we study the electronic properties of pristine and photo-chemically doped GO layers using field-effect transistor (FET) measurements.

Experimental

GO layer fabrication

Graphite oxide was synthesized by the modified Hummers method and exfoliated to give a brown dispersion of GO under ultrasonication. The resulting GO was negatively charged over a wide pH condition, as the GO sheet had chemical functional groups of carboxylic acids. GO solution in ethanol (0.5 mg mL^{-1}) at pH 3.3 was dropped after oxygen plasma treatment for 2 min in order to make the ITO surface hydrophilic. The GO solution was maintained for a waiting period of 2 min and was then spun at 3000 rpm for 30 s, followed by 30 min baking at 100 °C inside a nitrogen-filled glove box. The thickness of the films was analogous to the number of spinning repetitions; a film thickness of 3.4 nm was obtained with two successive coatings.

Photochemical doping of GO films

The as-spun GO layers on Si or PET substrates were subjected to irradiation by a KrF excimer laser source emitting 20 ns pulses of 248 nm at 1 Hz repetition rate that was translated onto the film area. For uniform exposure of the whole sample to laser radiation, a top-flat beam profile of 20 × 10 mm^2 was obtained using a beam homogenizer. The whole process took place in a vacuum chamber at 50 Torr Cl_2 or NH_3 gas pressure maintained through a precision micro-valve system. Different combinations of laser powers (P) and the number of pulses (N_p) were tested in an effort to optimize the photochemical functionalization processes. In a typical experiment, the sample was irradiated at a constant P with $N_p = 10$, 20, 30, 40, 50, 60, 120, 600 and 1200, corresponding to different photochemical reaction times.

Field effect transistor (FET) fabrication

Bottom-gate, bottom-contact FETs were initially prepared using pristine GO sheets. The transistor structures were fabricated using heavily doped p-type Si wafers acting as a common back-gate electrode and a 200 nm thermally grown SiO_2 layer as the gate dielectric. Using conventional photolithography, the gold source–drain (S–D) electrodes were defined with channel lengths and widths in the range 1–40 μm and 1–20 mm, respectively.

Microscopic and spectroscopic characterization

The morphology of the film surfaces was examined by atomic force microscopy (AFM; Digital Instruments NanoScope IIIa) (ESI, Fig. S1†). Fourier transform infrared (FTIR) spectra were recorded on a BRUKER FTIR spectrometer IFS 66v/F (MIR). Raman spectroscopy was performed using a Nicolet Almega XR Raman spectrometer (Thermo Scientific) with a 473 nm blue laser as an excitation source. X-ray photoelectron spectroscopy (XPS) measurements were carried out in a Specs LHS-10 Ultra-high Vacuum (UHV) system. The XPS spectra were recorded at room temperature using unmonochromatized Al Kα radiation under conditions optimized for the maximum signal (constant ΔE mode with a pass energy of 36 eV giving a full width at half maximum (FWHM) of 0.9 eV for the Au $4f_{7/2}$ peak). The analyzed area was an ellipsoid with dimensions 2.5 × 4.5 mm^2. The XPS core level spectra were analyzed using a fitting routine, which allows the decomposition of each spectrum into individual mixed Gaussian–Lorentzian components after a Shirley background subtraction. The ultraviolet photoelectron spectroscopy (UPS) spectra were obtained using HeI irradiation with $h\nu$ = 21.23 eV produced by a UV source (model UVS 10/35). During UPS measurements the analyzer was working at the Constant Retarding Ratio (CRR) mode, with CRR = 10. The work function was determined from the UPS spectra by subtracting their width (*i.e.* the energy difference between the analyzer Fermi level and the high binding energy cutoff), from the HeI excitation energy. For these measurements a bias of −12.30 V was applied to the sample in order to avoid interference of the spectrometer threshold in the UPS spectra. All the work function values obtained by UPS were calibrated using scanning Kelvin probe microscopy (SKPM) measurements. The relative error is 0.02 eV.

Results and discussion

The GO starting material used here was synthesized by a modified Hummers method.[29] The GO water dispersion was then spin coated directly onto silicon or PET[24] substrates.

Fig. 1 presents the irradiation scheme used for the realization of the doping process. The as-spun GO layers were

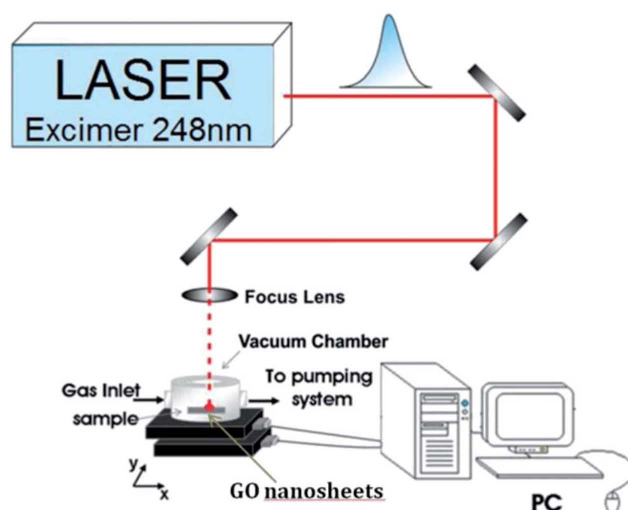

Fig. 1 Schematic of the experimental set-up used for the laser-induced doping of GO nanosheets.

 This journal is © The Royal Society of Chemistry 2014

subjected to irradiation by a KrF excimer laser source emitting 20 ns pulses of 248 nm at 1 Hz repetition rate that was translated onto the film area. For uniform exposure of the whole sample to laser radiation, a top-flat beam profile of 20 × 10 mm^2 was obtained using a beam homogenizer. The whole process took place in a vacuum chamber at 50 Torr Cl_2 or NH_3 gas pressure maintained through a precision micro-valve system. Different combinations of laser powers (P) and the number of pulses (N_p) were tested in an effort to optimize the photochemical functionalization processes. In a typical experiment, the sample was irradiated at a constant $P = 25$ mW with $N_p = 10$, 20, 30, 40, 50, 60, 120, 600 and 1200, corresponding to different photochemical reaction times. It should be noted here that the results are similar to those obtained upon irradiation with different intensities. Following irradiation, X-ray photoelectron spectroscopy (XPS) was used to probe and quantify the level of dopants introduced into the GO lattice. The respective measurements were carried out using a Kratos Axis Ultra spectrometer with an Al Kα monochromated X-ray beam at low pressures. Fig. 2a compares typical spectra of the pristine and Cl-doped GO. From these data it can be seen that the intensity of the O 1s peak relative to that of C 1s is reduced while the characteristic Cl 2p appears after irradiation. These results indicate laser-induced simultaneous reduction and Cl doping of the GO sheets. The Na peaks visible in the XPS scans are contributions from the sample mounting procedure and can therefore be ignored.

Analysis of the core level characteristic peaks allowed insight to be gained into the nature of the chemical bonds in each case. Fig. 2b and c present in high resolution the respective C 1s and Cl 2p peaks showing that, after irradiation, the C–O/C–C intensity ratio decreases from 1.09 to 0.60 while the Cl 2p/C 1s intensity ratio becomes equal to 0.17. In particular, the C 1s spectrum of as-prepared GO sheets showed a second peak at higher binding energies, corresponding to large amounts of sp^3 carbon with C–O bonds, carbonyls (C=O), and carboxylates (O–C=O),[30] resulted from harsh oxidation and destruction of the sp^2 atomic structure of graphene.

In our technique, by carefully tuning key laser parameters, the Cl-doping level could be readily controlled. An increase of P in the range from 10 to 50 mW or an increase of N_p at a certain P, gives rise to a corresponding decrease of the doping level. As shown in Fig. 3a, there is a rapid decrease of the Cl 2p/C ls ratio upon increasing N_p while at the same time a sharp increase in the GO reduction degree is evident. The maximum introduction

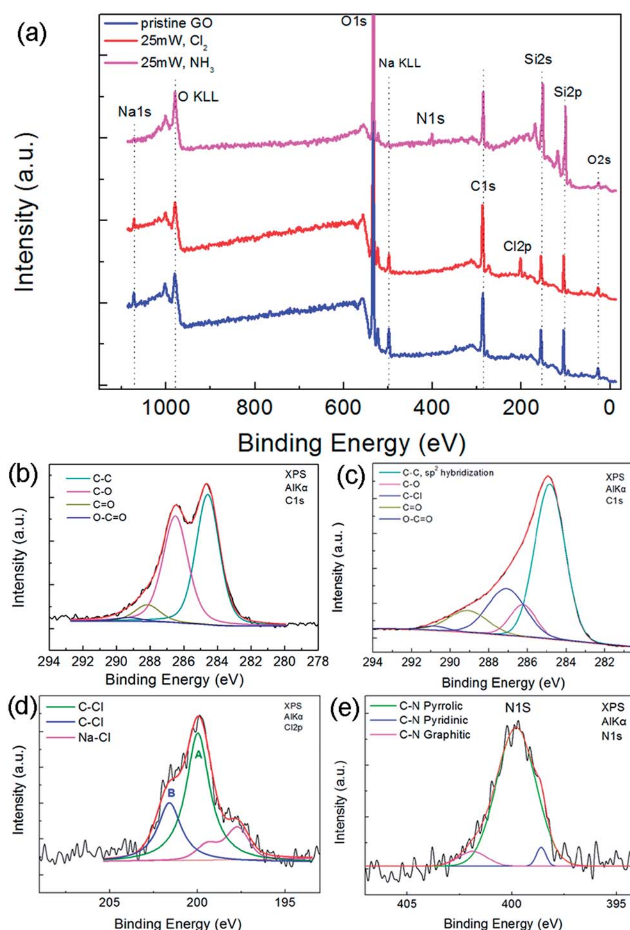

Fig. 2 (a) XPS survey spectra of pristine and laser treated GO in Cl_2 and NH_3; high-resolution XPS C 1s spectra of GO in its pristine (b) and laser treated in the Cl_2 (c) state; (d) high resolution Cl 2p XPS spectra of GO–Cl layers; (e) high resolution N 1s XPS spectra of GO–N layers.

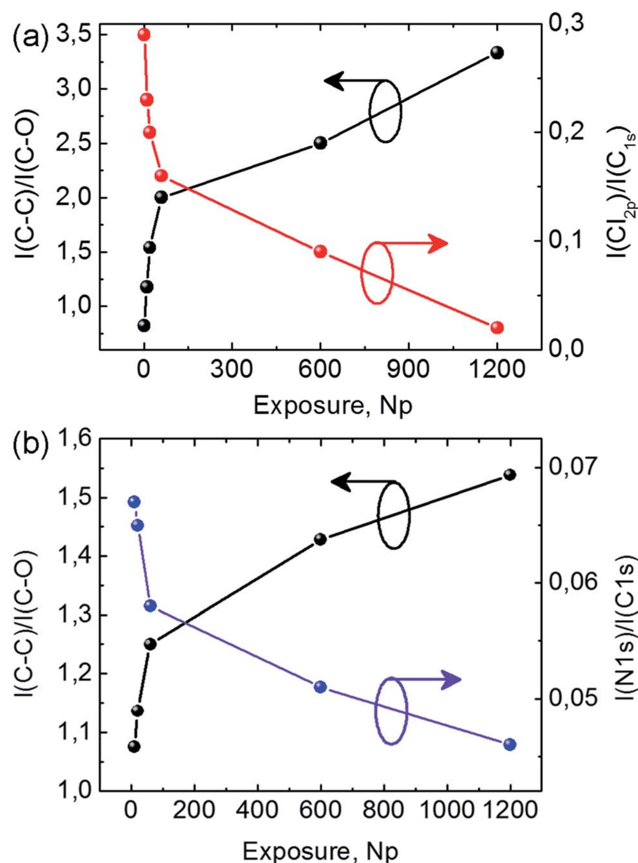

Fig. 3 (a) GO reduction and Cl doping levels as a function of the number of laser pulses, N_p; (b) GO reduction and N doping levels as a function of the number of laser pulses, N_p.

Published on 16 May 2014. Downloaded by University of Windsor on 22/08/2014 13:12:37.

Published on 16 May 2014. Downloaded by University of Windsor on 22/08/2014 13:12:37.

of Cl-groups attained was ~11.3 atom% as can be estimated by the ratio of the Cl 2p to the C 1s peak areas after considering the atomic sensitivity factors for Cl 2p and C 1s. We investigated the bonding configurations of Cl atoms in laser treated GO sheets based on high-resolution Cl 2p XPS spectra; a typical example is presented in Fig. 2d. In all cases, the Cl 2p peaks could be fitted into two peaks, one of lower energy, A ($2p_{3/2}$) and one of higher, B ($2p_{1/2}$). In all the samples, peak A was close to 200 eV and peak B near 201.7 eV corresponding to Cl–C at the edges and Cl–C=O groups, respectively.[31] The above findings indicate the enhancement of the doping efficiency upon increasing the number of the GO oxygen groups, suggesting that Cl-doping most likely occurs at the edges and defect sites.[32,33]

Similar results have been acquired using NH_3 gas as a precursor doping agent. The corresponding high resolution N 1S peak in Fig. 2e depicts that the nitrogen groups present in the N-doped graphene comprises a pyridinic (at ~398.6 eV), a pyrrolic (at ~399.8 eV) and a quaternary or graphitic nitrogen (at ~401.8 eV) peak.[16] Previous work attributed these contributions to the regions of pyridinic or pyrrolic peaks to the presence of amine groups.[15,16] The corresponding dependence of the N-doping level on N_p is presented in Fig. 3b. As in the case of Cl-doping oxygen groups existing at the edges and defect sites in the plane of GO react with NH_3, giving rise to N-doping, readily detected by XPS spectroscopy. The simultaneous reduction and N-doping of the GO nanolayers treated in NH_3 had been also confirmed *via* FTIR measurements (ESI, Fig. S1†). Following irradiation, the C=O and C–OH vibrational peaks were significantly reduced, while two characteristic new bands appeared at 1030 cm^{-1} and 1650 cm^{-1} due to the C–N bond stretch vibrations[34] and the bending mode of amide bonds[35] respectively.

Raman spectroscopy, one of the most sensitive techniques for the investigation of carbon based materials,[32] has been also used to investigate the effect of laser irradiation on the reduction and doping of the GO nanosheets. Fig. 4a depicts the respective spectra before and after laser irradiation in the presence of Cl_2. All spectra show the two prominent D (at ~1330 cm^{-1}) and G (at ~1590 cm^{-1}) bands, associated with carbon-based materials, corresponding to the degree of disorder and graphitization respectively.[36,37] Also, the presence of a weak 2D band is typical for chemically derived graphene. Although this band was not altered appreciably with the exposure time, the D and G bands were observed to change upon increasing the number of laser pulses, as shown in the inset of Fig. 4a. In particular, the intensity ratio of the D to G bands (I_D/I_G), which is commonly used as a measure of defect levels in graphene, is seen to progressively increase with exposure time ($I_D/I_G \sim 0.88$ before laser treatment and 0.95 after laser treatment (Fig. 4b)). It had been found that, an increase of the I_D/I_G ratio in GO indicates lattice disordering or ordering depending on the starting defect levels. Based on the measured decrease in channel conductance of the laser-doped GO transistors presented below the increase of the I_D/I_G ratio can be attributed to an increase in defects and disorder in laser treated samples, associated with the decrease in the sp^2-C content as well as the presence of the Cl–C=O form. Furthermore, both peaks gradually shift to higher wavenumbers upon increasing the number

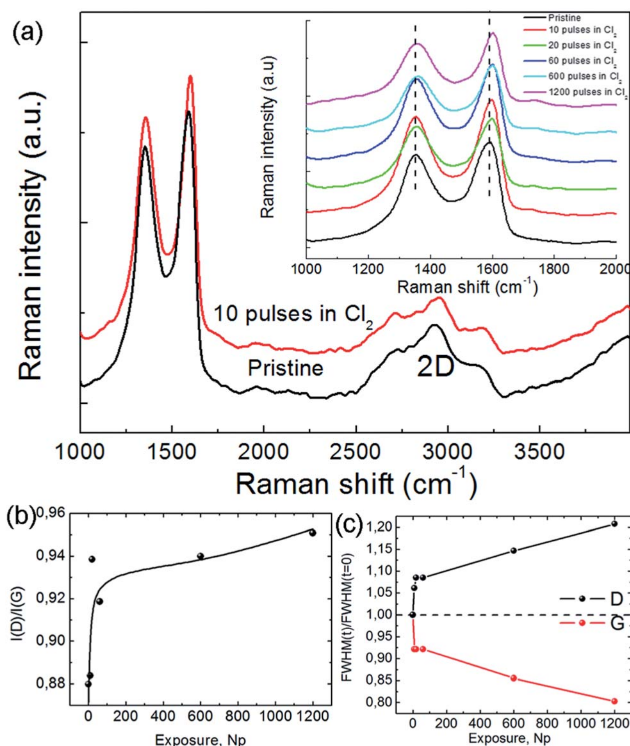

Fig. 4 (a) Micro-Raman measurements of GO sheets before (pristine) and after irradiation with 10 laser pulses in Cl_2; the evolution of the G and D bands with different numbers of pulses is presented in the inset; (b) dependence of the I_D/I_G ratio on the number of the laser pulses, N_p; (c) dependence of the D and G band's FWHM (normalized values) on N_p.

of pulses, with the G peak shifting by ~10 cm^{-1}, while the D by ~4 cm^{-1} (ESI, Fig. S2†). The observed blue shift of the G-band position has been attributed to phonon stiffening with doping of GO.[38,39] Moreover, as shown in Fig. 4c, the G band becomes narrower while at the same time the D band gets broader with increasing exposure time. The D line broadening complies with the I_D/I_G ratio increase and can be attributed to the enhancement of GO reactivity as more defect sites are created.[40] On the other hand, the G band narrowing may be attributed to the doping effect suggesting that covalent bonds, C–Cl bonds, were formed and thus a transformation of the sp^2 type C–C bonds to sp^3 had been induced.[9] The saturation effect observed for I_D/I_G, G and D peak positions and FWHM after illumination with 60 pulses complies with the trend of saturation in the doping efficiency observed in the respective XPS spectra (*i.e.* compare Fig. 2 and 4). Based on the above XPS and Raman analyses, it can be concluded that the reduction and doping levels can be readily controlled by increasing the laser exposure time. Most important, XPS measurements reveal that the laser induced dopants are stable for months upon sample storage under ambient conditions.

Concerning the mechanism behind laser-induced doping, it can be postulated that upon excitation with UV laser pulses, chlorine and nitrogen radicals are generated in the gas phase *via* photodissociation of Cl_2 and NH_3 precursor gases respectively.[41] Subsequently, the radicals formed preferentially react

 This journal is © The Royal Society of Chemistry 2014

Published on 16 May 2014. Downloaded by University of Windsor on 22/08/2014 13:12:37.

with the GO lattice *via*, thermodynamically favorable, free radical addition reactions.[11,21] At the same time, electrons generated under irradiation can be captured by GO hence leading to GO reduction.[42] Further investigations are currently in progress to explore and understand the exact mechanism behind the laser-induced doping process.

To investigate how N- and Cl-doping affect the microscopic electronic properties of graphene, bottom-gate, bottom-contact FETs were initially prepared using pristine GO sheets. The transistor structures were fabricated using heavily doped p-type Si wafers acting as a common back-gate electrode and a 200 nm thermally grown SiO_2 layer as the gate dielectric (Fig. 5a and b). Using conventional photolithography, the gold source–drain (S–D) electrodes were defined with channel lengths and widths in the range 1–40 μm and 1–20 mm, respectively. The GO flakes were deposited by dip-coating at room-temperature directly onto 1.5 cm × 1.5 cm size substrates containing few hundreds of pre-patterned S–D electrode pairs. The samples were then thermally annealed at 200 °C in nitrogen. As-prepared devices were subjected to *in situ* laser irradiation under identical conditions used for the experiments performed on nanolayers.

Fig. 5c and d show the channel transconductances (G) *versus* gate voltage (V_G) characteristics of two GO transistors before and after laser irradiation in the presence of Cl_2 and NH_3 gases, respectively. For the annealed GO devices (pristine) the G–V_G plot shows the typical 'V' shaped ambipolar transfer characteristic[7] with a distinct asymmetry in the electron and hole branches. The charge neutrality point (CNP) for the pristine GO devices was found to vary between 2 V and −12 V. The often measured positive values for the DP indicate unintentional p-doping, probably caused by oxygen species physisorbed on the surface/edges of the GO layers during device preparation.[28] In order to study the impact of laser irradiation in the presence of different dopant gases on the transport properties of GO channels, the transfer curves for each device were recorded prior to and after laser irradiation with and without the dopant gas presence. To ensure the validity of the changes in the transfer curves following the doping process, the laser treatment was performed *in situ* in postfabricated transistors. In a typical experiment the pristine transfer curve of a transistor based on undoped GO was recorded followed by laser treatment in the presence of the dopant precursor gas. Afterwards, the new transfer curve was measured and compared to that obtained in the pristine state. In the time periods among the measurements, the transistor was kept in an inert atmosphere in order to avoid unintentional doping due to physisorbed atoms and molecules.

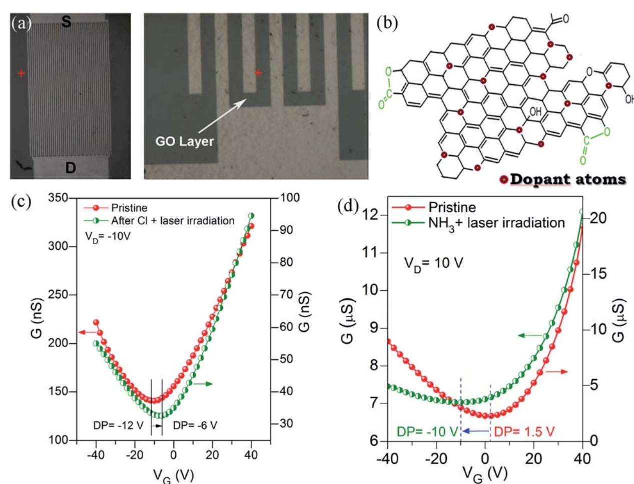

Fig. 5 (a) Optical microscopy images of GO FETs; (b) schematic representation of reduced and doped GO lattices; (c) transfer characteristics measured for FETs based on rGO before (pristine) and after exposure of the channel to Cl and laser irradiation (Cl_2 + laser irradiation); (e) transfer characteristics measured for FETs based on rGO before (pristine) and after exposure of the channel to NH_3 and laser irradiation (NH_3 + laser irradiation). DP corresponds to the charge neutrality point.

Laser treatment in the presence Cl_2 gas leads to a drop in the overall channel conductance under both p- and n-channel operation. The clear shift in the CNP to more positive voltages is most likely the result of the enhanced p-type conductivity of the GO channel due to the photochemically induced p-type doping of GO.[7,43] This observation is in qualitative agreement with the shift in the work function (WF) of the GO layer from 4.91 eV to 5.23 eV measured before and after laser irradiation, respectively (ESI, Fig. S3a†). Laser irradiation of the control samples under an inert atmosphere is found to have no distinguishable impact on the transporting characteristics of the device (ESI, Fig. S3b†). Based on these results we conclude that the observed changes in the channel conductance can only be attributed to p-doping caused primarily by laser induced photoreaction with the dopant gas (Cl_2).

When the GO channel was irradiated with laser light in the presence of NH_3 (Fig. 5d), the device characteristics exhibit the opposite trend to that seen in transistors irradiated in the presence of Cl_2 gas (Fig. 5c). In particular, the CNP is found to shift to more negative gate voltages indicative of n-type doping.[44] This observation is in good agreement with the measured shift in the WF function from 4.91 eV for the pristine GO to 4.6 eV for laser irradiated GO in the presence of NH_3 (ESI, Fig. S3b†). Table 1 summarizes the respective on/off ratios and mobility values for GO transistors treated in Cl_2 and NH_3 respectively. It is clear that the photochemical process is rapid, since a few nanosecond pulses in the presence of a reactive dopant gas are sufficient to induce up to a five-fold increase of the channel on/off ratio.[9] In contrast to the WF changes described above, the relatively small change of the on/off ratio indicates a minor electronic effect due to dopant atoms.

Table 1 Carrier mobilities and on/off ratios of GO transistors subjected to laser treatment in Cl_2 and NH_3 respectively

	μ_{lin} [$cm^2 V^{-1} s^{-1}$]		I_{ON}/I_{OFF}	
Sample	Before irradiation	After irradiation	Before irradiation	After irradiation
Laser treated in NH_3 (50 mJ, 10 pulses)	3.10×10^{-3}	9.83×10^{-4}	2.25	8.91
Laser treated in Cl_2 (50 mJ, 10 pulses)	16.3×10^{-3}	3.81×10^{-3}	1.53	3.61

View Article Online

Published on 16 May 2014. Downloaded by University of Windsor on 22/08/2014 13:12:37.

The general decrease in GO conductivity (holes and electrons) observed upon photochemical doping suggests an increase in the structural disorder, which is in agreement with the Raman measurements presented above. Such lattice disorder could be caused either by interruption of the conjugated system or the introduction of scattering centers.[45,46] The decrease in both electron and hole mobilities together with the G-band narrowing is the indication that the laser induced photochemical reaction(s) gives rise to substitutional doping at the expense of surface charge transfer doping.[9] This observation is in contrast to the increase in carrier mobility and improvement in the lattice order observed upon laser treatment of GO under an inert atmosphere.[26] The present results confirm that laser irradiation of GO under an inert atmosphere does not induce any structural disorder and the presence of reactive dopant gas(es) combined with laser irradiation is the main reason for the observed doping effects.

Conclusions

Based on the results presented here it can be concluded that laser irradiation in the presence of a reactive gas can be used as an easy and catalyst-free approach for the synthesis of doped GO derivatives. The proposed method is simple and provides access to controllable reduction and doping of GO at room temperature hence allowing the combination of the technique with temperature sensitive substrate materials such as plastic. The rather simple and scalable method could potentially be used for the synthesis of novel graphene-based derivatives that are difficult or impossible to obtain *via* conventional synthetic routes.

Acknowledgements

This work was performed in the framework of the PROENYL research project, Action KRIPIS, project No MIS-448305 (2013SE01380034) that was funded by the General Secretariat for Research and Technology, Ministry of Education, Greece and the European Regional Development Fund (Sectoral Operational Programme: Competitiveness and Entrepreneurship, NSRF 2007-2013)/European Commission. The authors acknowledge Ms Labrini Syggelou from FORTH-ICEHT for her support with the XPS/UPS measurements.

Notes and references

1 K. S. Novoselov, A. K. Geim, S. V. Morozov, D. Jiang, Y. Zhang, S. V. Dubonos, I. V. Grigorieva and A. A. Firsov, *Science*, 2004, **306**, 666–669.
2 A. Geim and K. S. Novoselov, *Nat. Mater.*, 2009, **324**, 1530–1534.
3 S. Yu, W. Zheng, C. Wang and Q. Jiang, *ACS Nano*, 2010, **4**, 7619–7629.
4 F. Schedin, A. K. Geim, S. V. Morozov, E. W. Hill, P. Blake, M. I. Katsnelson and K. S. Novoselov, *Nat. Mater.*, 2007, **6**, 652–655.
5 C. Casiraghi, *Phys. Rev. B: Condens. Matter Mater. Phys.*, 2009, **80**, 233407.
6 B. Guo, L. Fang, B. Zhang and J. R. Gong, *Insci. J.*, 2011, **1**, 80–89.
7 Z. Luo, N. J. Pinto, Y. Davila and A. T. C. Johnson, *Appl. Phys. Lett.*, 2012, **100**, 1–4.
8 E. Bekyarova, M. E. Itkis, P. Ramesh, C. Berger, M. Spinkle, W. A. de Heer and R. C. Haddon, *J. Am. Chem. Soc.*, 2009, **131**, 1336.
9 H. Liu, Y. Liu and D. Zhu, *J. Mater. Chem.*, 2011, **21**, 3335–3345.
10 D. C. Elias, R. R. Nair, T. M. G. Mohiuddin, S. V. Morozov, P. Blake, M. P. Halsall, A. C. Ferrari, D. W. Boukhvalov, M. I. Katsnelson and A. K. Geim, *Science*, 2009, **323**, 610–613.
11 B. Li, L. Zhou, D. Wu, H. Pang, K. Yan, Y. Zhou and Z. Liu, *ACS Nano*, 2011, **5**, 5957–5961.
12 L. Zhang, S. Diao, Y. Nie, K. Yan, N. Liu, B. Dai, Q. Xie, A. Riena, J. Kong and Z. Liu, *J. Am. Chem. Soc.*, 2011, **133**, 2706–2713.
13 L. Zhang, Y. Ye, D. Cheng, W. Zhang, H. Pan and J. Zhu, *Carbon*, 2013, **62**, 365–373.
14 P. Gong, Z. Wang, Z. Li, Y. Mi, J. Sun, L. Niu, H. Wang, J. Wang and S. Yang, *RSC Adv.*, 2013, **3**, 6327.
15 X. Li, H. Wang, J. T. Robinson, H. Sanchez, G. Diankov and H. Dai, *J. Am. Chem. Soc.*, 2009, **131**, 15939–15944.
16 N. Ashok Kumar, H. Nolan, N. McEvoy, E. Reznavi, R. Doyle, M. Lyons and G. Duesberg, *J. Mater. Chem.*, 2013, **1**, 4431–4435.
17 T. N. Huan, T. V. Khai, Y. Kang, K. B. Shimb and H. Chung, *J. Mater. Chem.*, 2012, **22**, 14756–14762.
18 Y. Liu, N. Tang, X. Wan, Q. Feng, M. Li, Q. Xu, F. Liu and Y. Du, *Sci. Rep.*, 2013, **3**, 2566.
19 G. Singh, D. S. Sutar, V. Divakar Botcha, P. K. Narayanam, S. S. Talwar, R. S. Srinivasa and S. S. Major, *Nanotechnology*, 2013, **24**, 355704.
20 S. Wang, P. J. Chia, L. L. Chua, L. H. Zhao, R. Q. Png, S. Sivaramakrishnan, M. Zhou, R. G. S. Goh and R. H. Friend, *Adv. Mater.*, 2008, **20**, 3440.
21 H. Liu, S. Ryu, Z. Chen, M. L. Steigerwald, C. Nuckolls and L. E. Brus, *J. Am. Chem. Soc.*, 2009, **131**, 17099–17101.
22 Y.-L. Zhang, L. Guo, H. Xia, Q.-D. Chen, J. Feng and H.-B. Sun, *Adv. Opt. Mater.*, 2014, **2**, 10.
23 Y. Zhang, L. Guo, S. Wei, Y. Hec, H. Xia, Q. Chen, H.-B. Sun and F.-S. Xiao, *Nano Today*, 2010, **5**, 15.
24 E. Kymakis, K. Savva, M. M. Stylianakis, C. Fotakis and E. Stratakis, *Adv. Funct. Mater.*, 2013, **23**, 2742–2749.
25 L. Guo, R.-Q. Shao, Y.-L. Zhang, H.-B. Jiang, X.-B. Li, S.-Y. Xie, B.-B. Xu, Q.-D. Chen, J.-F. Song and H.-B. Sun, *J. Phys. Chem. C*, 2012, **116**, 3594.
26 C. Petridis, Y.-H. Lin, K. Savva, G. Eda, E. Kymakis, T. D. Anthopoulos and E. Stratakis, *Appl. Phys. Lett.*, 2013, **102**, 093115.
27 L. Guo, Y.-L. Zhang, D.-D. Han, H.-B. Jiang, D. Wang, X.-B. Li, H. Xia, J. Feng, Q.-D. Chen and H.-B. Sun, *Adv. Opt. Mater.*, 2014, **2**, 120.
28 T. O. Wehling, K. S. Novoselov, S. V. Morozov, E. E. Vdovin, M. I. Katsnelson, A. K. Geim and A. I. Lichnenstein, *Nano Lett.*, 2008, **8**, 173–177.

This journal is © The Royal Society of Chemistry 2014

Published on 16 May 2014. Downloaded by University of Windsor on 22/08/2014 13:12:37.

29 Z. Luo, Y. Lu, L. A. Somers and A. T. C. Johnson, *J. Am. Chem. Soc.*, 2009, **131**, 898–899.

30 S. Stankovich, D. A. Dikin, R. D. Piner, K. A. Kohlhaas, A. Kleinhammes, Y. Y. Jia, Y. Wu, S. T. Nguyen and R. S. Ruoff, *Carbon*, 2007, **45**, 1558–1565.

31 D.-W. Wang, K.-H. Wu, I. R. Gentle and G. Q. Lu, *Carbon*, 2012, **50**, 333.

32 X. Wang, X. Li, L. Zhang, Y. Yoon, P. K. Weber, H. Wang, J. Guo and H. Dai, *Science*, 2009, **324**, 768–771.

33 J. L. Bahr, J. P. Yang, D. V. Kosynkin, M. J. Bronikowski, R. E. Smalley and J. M. Tour, *J. Am. Chem. Soc.*, 2001, **123**, 6536–6542.

34 T. Ramanathan, F. T. Fisher, R. S. Ruoff and L. C. Brinson, *Chem. Mater.*, 2005, **17**, 1290.

35 N. Karousis, S. P. Economopoulos, E. Sarantopoulou and N. Tagmatarchis, *Carbon*, 2010, **48**, 854.

36 A. C. Ferrari, *Solid State Commun.*, 2007, **143**, 47–57.

37 D. Zhan, Z. H. Ni, W. Chen, L. Sun, Z. Q. Luo and L. F. Lai, *Carbon*, 2011, **49**, 1362–6.

38 M. A. Pimenta, G. Dresselhaus, M. S. Dresselhaus, L. G. Cancado, A. Jorio and R. Saito, *Phys. Chem. Chem. Phys.*, 2007, **9**, 1276.

39 A. Das, S. Pisana, B. Chakraborty, S. Piscanec, S. K. Saha, U. V. Waghmare, K. S. Novoselov, H. R. Krishnamurthy, A. K. Geim, A. C. Ferrari and A. K. Sood, *Nat. Nanotechnol.*, 2008, **3**, 210.

40 H. Liu, S. Ryu, Z. Chen, M. L. Steigerwald, C. Nuckolls and L. E. Brus, *J. Am. Chem. Soc.*, 2009, **131**, 17099–17101.

41 H. Sato, *Chem. Rev.*, 2001, **101**, 2687–2726.

42 Y. Matsumoto, M. Koinuma, S. Ida, S. Hayami, T. Taniguchi, K. Hatakeyama, H. Tateishi, Y. Watanabe and S. Amano, *J. Phys. Chem. C*, 2011, **115**, 19280–19286.

43 G. Eda, Y.-Y. Lin, S. Miller, C.-W. Chen, W.-F. Su and M. Chhowalla, *Appl. Phys. Lett.*, 2008, **92**, 233305.

44 Y.-C. Lin, C.-Y. Lin and P.-W. Chiu, *Appl. Phys. Lett.*, 2010, **96**, 133110.

45 G. Eda, A. Nathan, P. Wobkenberg, F. Colleaux, K. Ghaffarzadeh, T. Anthopoulos and M. Chhowalla, *Appl. Phys. Lett.*, 2013, **102**, 133108.

46 D. C. Elias, R. R. Nair, T. M. Mohiuddin, S. V. Morozov, P. Blake, M. P. Halsall, A. C. Ferrari, D. W. Bouchvalov, M. I. Katsnelson, A. K. Geim and K. S. Novoselov, *Science*, 2009, **323**, 610–613.